# Energetic and exergetic evaluation of the hybridization of Solar Combined Cycle Power Plants

**Sotirios Karellas[1], Soteris Kalogirou[2], Anastasios Lappas[1], Athanasios Papadopoulos[1], Emmanuel Kakaras[1]**

[1] *Laboratory of Steam boilers and Thermal Plants, National Technical University of Athens, 9 Heroon Polytechniou Str. 15780, Zografou, Athens, Greece*

[2] *Archimedes Solar Energy Laboratory, Department of Mechanical Engineering and Materials Sciences and Engineering, Cyprus University of Technology, P. O. Box 50329, 3603 Lemessos, Cyprus*

**Keywords**: Integrated Solar Combined Cycle (ISCC), Solar Tower, Combined Cycle, hybridization, Thermal Energy Storage (TES)

**Abstract:** The economic crisis, high fuel prices, high generation costs, environmental considerations and international guidelines on carbon emissions have been a strong driver for the increasing exploitation of the use of renewable energy, or hybridization of fossil fired plans. The high levels of Direct Normal Irradiance (DNI) of these countries led them to consider hybridizing existing power plants with concentrated solar energy, substituting natural gas or diesel oil. The Integrated Solar Combined Cycle System (ISCCS) is one of the most promising hybrid configurations for substitution of part of the fossil fuel by efficiently converting solar energy into electricity.

The scope of this paper is to simulate and compare energetically and exergetically the potential of hybridizing two Combined Cycle Power Plants (CCPP) in different areas of the Mediterranean region. The plant considered is located in Thisvi, Voiotia, Greece, and is natural gas-fired and is owned and operated by Elpedison.

The Concentrating Solar Power technology (CSP) which was chosen to integrate the above mentioned Combined Cycle is basically a solar tower using molten salt as working fluid. The designed solar field layout is based on a methodology presented on recent published studies and the final computations are performed with the IPSEpro software. This study takes into account a wide range of parameters such as different tower heights, heliostat field layouts, heliostat dimensions and DNI values. In addition, a Thermal Energy Storage (TES) configuration was considered, in order to store the excessive solar thermal energy and deliver it back during the absence of irradiation.

In conclusion, an economic analysis is conducted and indicates that there are substantial gains to be obtained in ISCC plants through solar contribution, both in power plant efficiency and fuel savings.

---

Contents

5. Economic evaluation of the investment

6. Conclusions

| Nomenclature | | | |
|---|---|---|---|
| CCPP | Combined Cycle Power Plant | NPV | Net Present Value |
| CCGT | Combined Cycle Gas Turbine | GHI | Global Horizontal Irradiance |
| ISCC | Integrated Solar Combined Cycle | CSP | Consentrated Solar Power |
| TES | Thermal Energy Storage | PV | Present Value |
| DNI | Direct Normal Iradiance | LEC | Levelized Electricity Cost |
| SH | Super Heater | GT | Gas Turbine |
| EVAP | Evaporator | ST | Steam Turbine |
| ECO | Economizer | LP | Low Pressure |
| PRH | Preheater | HRSG | Heat Recavery Steam Geneator |
| HP | High Pressure | IRR | Internal Rate of Return |
| MP | Medium Pressure | DSG | Direct Steam Generation |
| LP | Low Pressure | HTF | Heat Transfer Fluid |
| LEC | Levelised Electricity Cost | | |

## 1. Introduction

During the last 50 years developing European countries, such as Greece and Cyprus, had to deal with fast-growing energy demands. This led to the design of high efficiency and quick installation power plants. The most commonly installed technology was Combined Cycle Gas Turbine (CCGT), which proved to be one of the most efficient energy conversion systems. Whereas the last couple decades, the EU has shown great interest in environmental-friendly technologies and green energy production. Cyprus and Greece are required to meet the EU environmental standards, which means that by 2020, 20 % of their energy consumption must come from renewable sources and greenhouse gases emissions (CO2 especially) must be reduced by 20%. Under these standards, we study the possible hybridization of existing CCP with CSP technology.

Integrated Solar combined cycle systems (ISCC) are modern combined cycle power plants with gas and steam turbines and additional thermal input of solar energy from a solar receiver system [1]. ISCC plants offer some principal advantages: firstly, solar energy can be converted to electric energy at a higher efficiency [2]. Secondly, studies have shown that solar hybridization into an NGCC plant may give rise to a substantial benefit from a thermodynamic point of view [3,4]. Integrated Solar Combined Cycles (ISCCs) allow lower fossil fuel consumption and lower CO2 emissions than conventional combined cycles, as well as a rational use of local and renewable resources[5]. Besides, ISCCs reach higher solar-to electricity conversion efficiency than conventional STPPs, since they are based on a more efficient technology and, at the same time, they avoid the need of thermal storage, reduce the generation costs and allow advancing in the learning curve with minimum operational risk [4] .

An ISCC plant needs high solar thermal input to make the investment worthwhile. The average annual distribution of DNI in EU countries is presented on Figures 1 and Table 1a&1b. The mean

values of GHI and DNI potential of Greece are 1637 kWh/m$^2$ and 1576 kWh/m$^2$ respectively. Cyprus has even higher values, with annual GHI potential around 1902 kWh/m$^2$ and annual DNI potential 1968 kWh/m$^2$ [6]. The difference in the above values is due the geographical position of the island of Cyprus. Nonetheless, these values are well above the average values of the rest European countries (table 1a&1b), so both countries are major candidates for appliance of CSP technology. In Greece, annual solar radiation increases from north to south and from the continental parts towards the coast. Cyprus has high solar radiation during the whole year with mean daily sunshine of 5.5 hours during winter and 12.5 hours during summer [7].

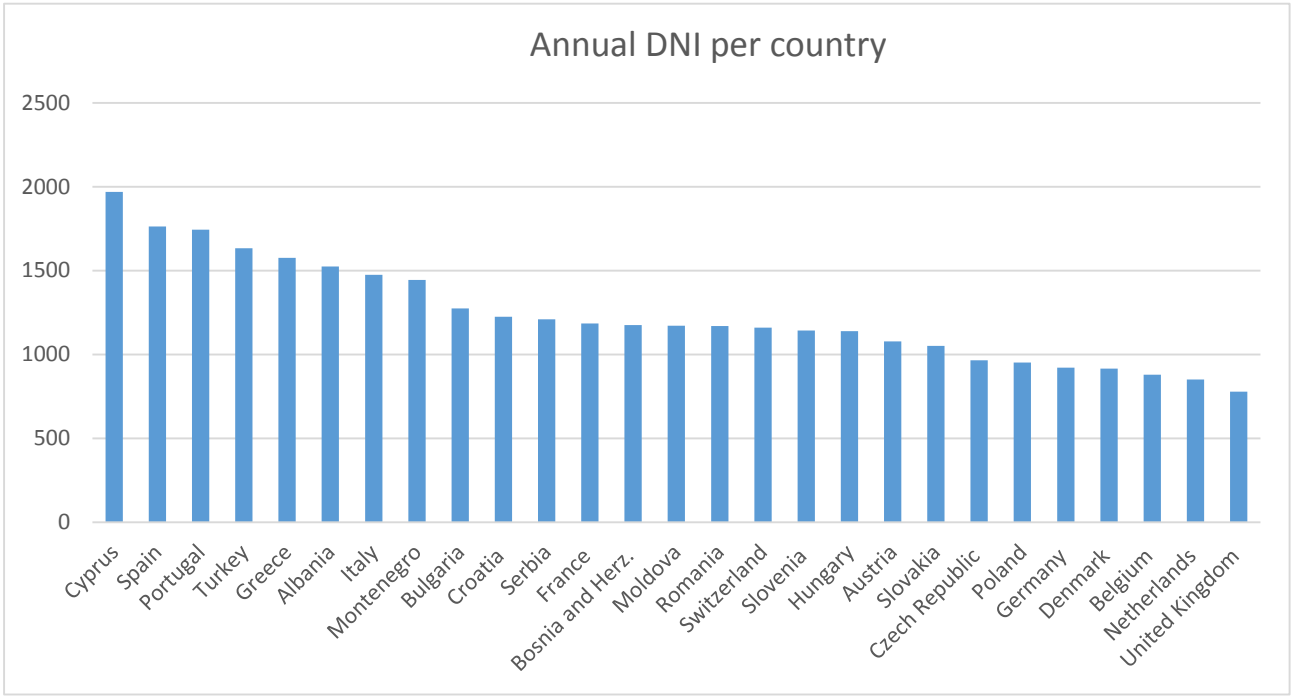


*Figure 1a. Annual DNI of European Countries*

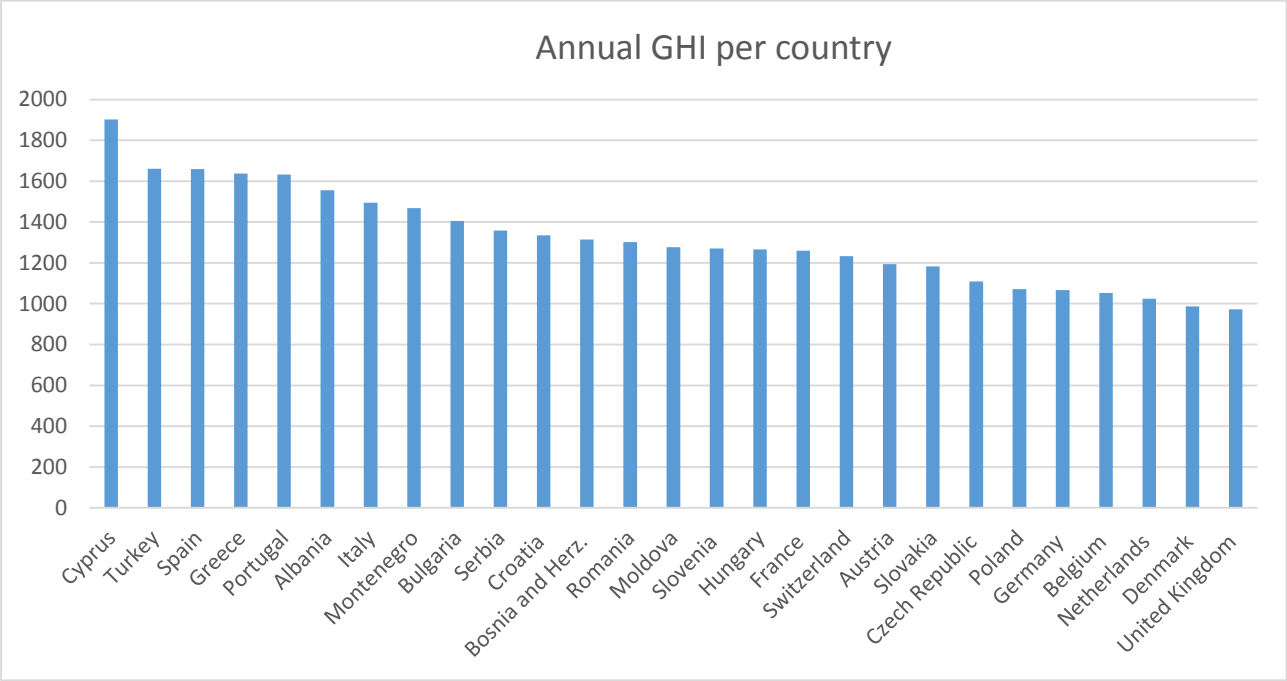


*Figure 1b. Annual GHI of European Countries*

## 2. Plant Description

A typical NGCC plant consists of gas turbines, steam turbines and a heat recovery steam generation system (HRSGs) with an optional duct burner [4].The performance of each of these components is strictly dependent on that of the others. Accurate simulation of such power plants requires sophisticated software programs, designed for power cycle simulations, such as the IPSEpro which is used in this study.

IPSEpro allowed us to simulate several solar tower models and solar integration was studied in three different stages of the plant. By using IPSEpro a detailed thermodynamic modeling of our NGCC plant with solar integration was achieved, while additional components, such as the heliostat field and solar tower, were designed with IPSEpro's model development kit (MDK).

The NGCC plant studied in this paper is illustrated in Figure 2a and 2b. The plant includes a gas turbine, a duct burner, a HRSG system and a steam turbine. The steam turbine includes three pressure stages: high pressure (HP), middle pressure (MP) and low pressure (LP). The HRSG utilizes the flue gas and the additional heating (if needed) from the gas turbine and the duct burner respectively, to heat the feed water to the high-pressure, high-temperature steam feeding into the steam turbine, through a series of superheaters, evaporators and economizers.

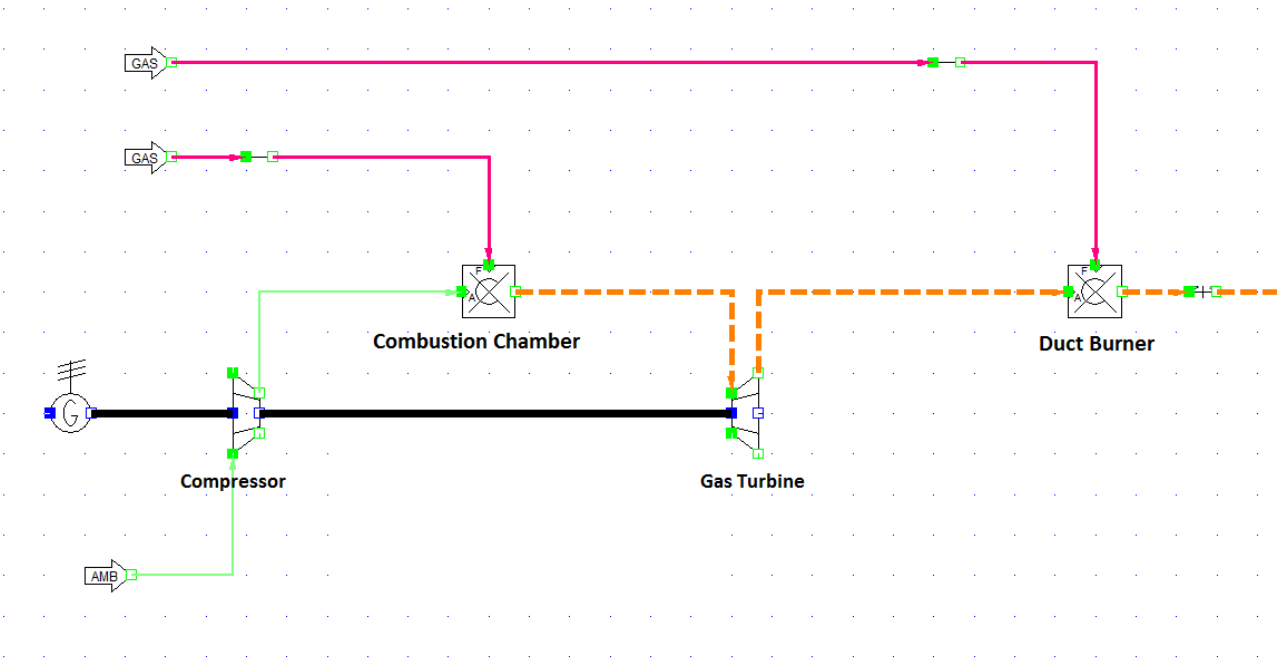


*Figure 2a. Gas Turbine, Compressor, Combustion chamber and Duct burner*

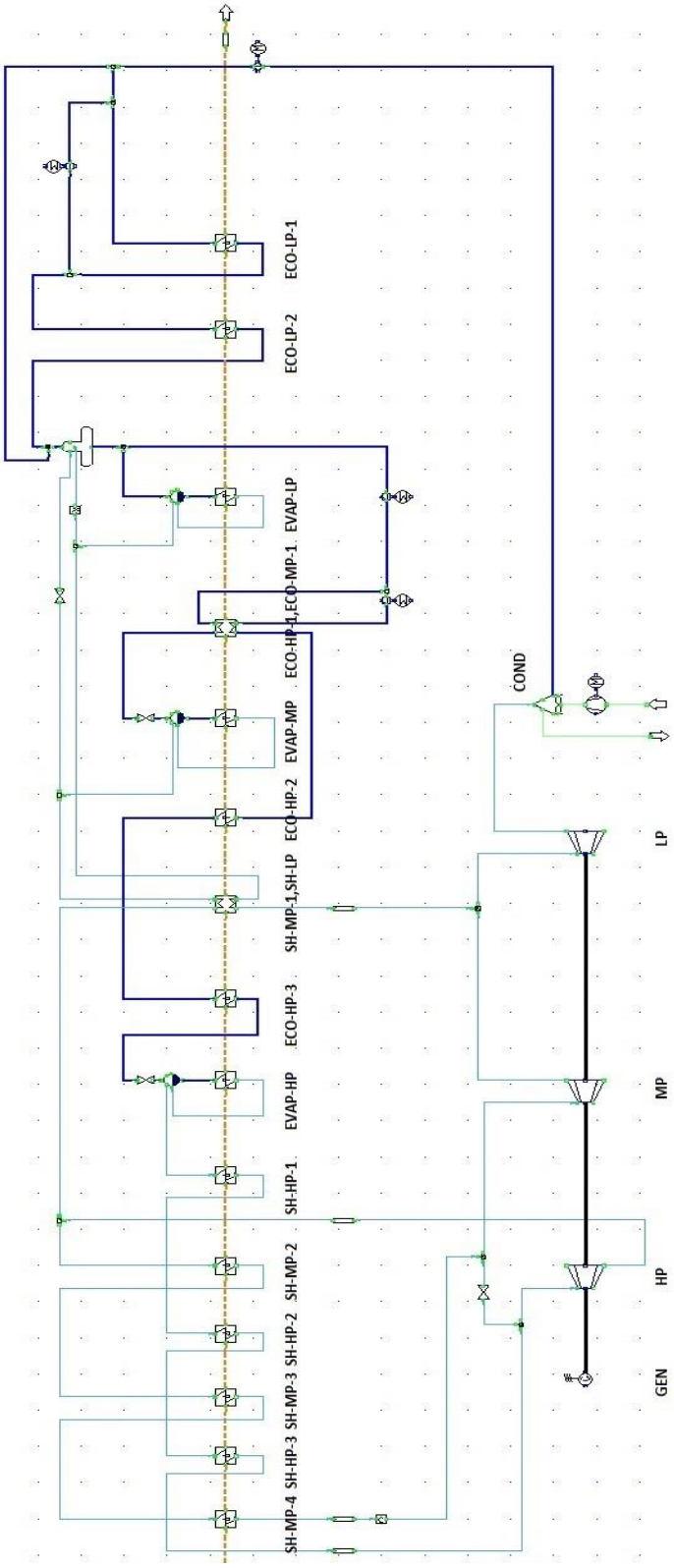


*Figure 2b. Heat Recovery Steam Generation System*

At its present state (before the solar thermal input), the performance of the plant's major components are listed in table 2.

*Table 2. Performance values of NGCC plant's components*

| Component | Values | Units |
|---|---|---|
| **Overall Plant** | | |
| Nominal Ambient Pressure | 1 | bar |
| Nominal Ambient Temperature | 15 | °C |
| Gas Turbine | 1 | - |
| HRSG | 1 | - |
| Steam Turbine | 1 | - |
| Duct Burner | Yes | - |
| Cooling | Dry | - |
| Total Capacity | 407.3 | MWe |
| Overall Efficiency | 57.93 | % |
| **Gas Turbine** | | |
| Nominal Power Output | 275.2 | MWe |
| Nominal Efficiency | 39.14 | % |
| Outlet Temperature | 1375 | °C |
| Pressure Ratio | 33.92 | % |
| **Steam Turbine** | | |
| Nominal Power Output | 132 | MWe |
| Nominal Cycle Efficiency | 18.79 | % |
| HP Steam Mass Flow rate | 71.8 | kg/s |
| HP Inlet Temperature | 550.89 | °C |
| HP Inlet Pressure | 119.35 | bar |
| MP Steam Mass Flow rate | 84.63 | kg/s |
| MP Inlet Temperature | 547.93 | °C |
| MP Inlet Pressure | 29.35 | bar |
| LP Steam Mass Flow rate | 97.84 | kg/s |
| LP Inlet Temperature | 281.67 | °C |
| LP Inlet Pressure | 4.04 | bar |
| LP Outlet Temperature | 39 | °C |
| LP Outlet Pressure | 0.07 | bar |
| **HRSG** | | |
| Flue Gas Mass FlowRate | 669.6 | kg/s |
| Flue Gas Inlet Temperature | 574.98 | °C |
| Flue Gas Outlet Temperature | 103.94 | °C |

The steam/water current gradually raises its temperature as it goes through the HRSG system and gains heat from the flue gas current. The heat transaction taking place is presented in figure 3. The HRSG system consists of seven HP heat exchangers, six MP heat exchangers and four LP heat exchangers. One thing worth mentioning, is the existence of a dual-pressure economizer, named

ECO-HP1,ECO-MP1 for HP and MP feedwater heating, as well as a dual pressure superheater for MP and LP feedwater heating (named SH-MP1,SH-LP).

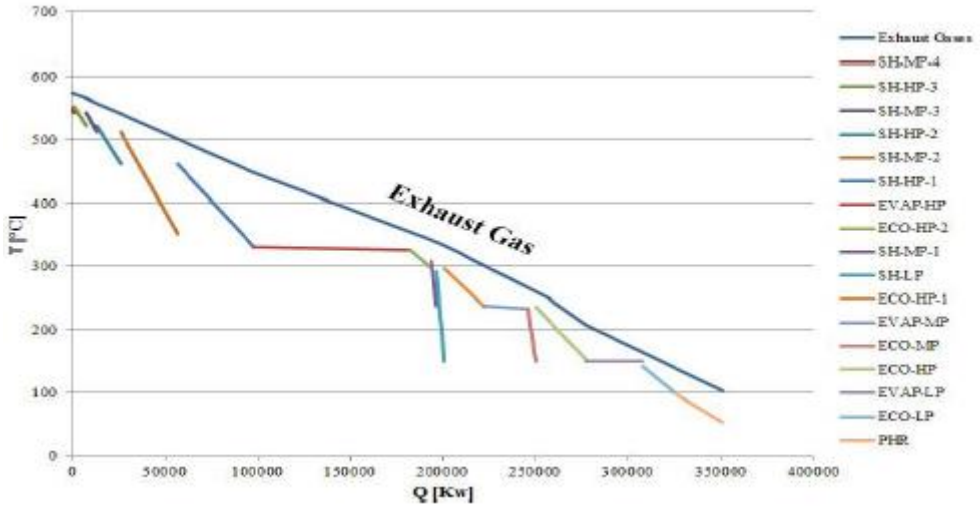


*Figure 3. Q-T Diagram of steam/water and gas current*

As the title of the paper suggests, an exergetic analysis of the plant was also carried out. Exergy of a thermodynamic system is the maximum theoretical useful work (shaft work or electrical work) obtainable as the system is brought into complete thermodynamic equilibrium with the thermodynamic environment while the system interacts with this environment only.

The Sankey and Grassmann diagrams illustrated below show the energy flow and exergy destruction respectively (before the solar integration).

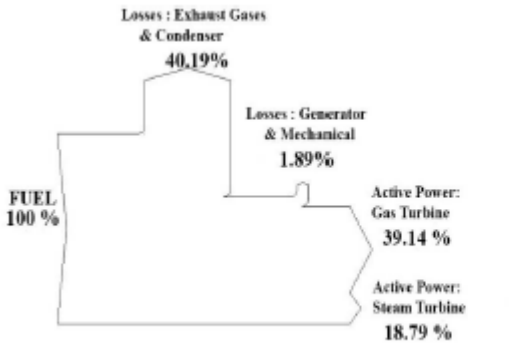


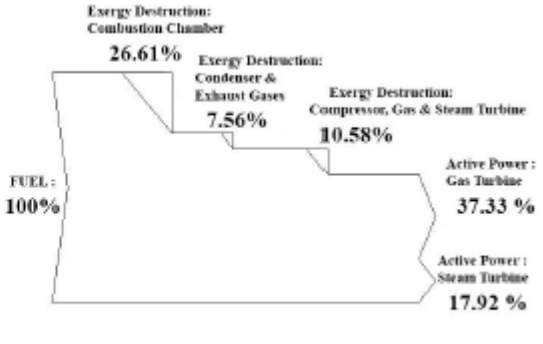


*Figure 4a. Sankey Diagram*

*Figure 4b. Grassmann Diagram*

## 3. Heliostat Field

CSP technology consists of systems that concentrate the beam radiation of the sun to produce high-temperature thermal energy for various uses. Today the focus is on utility-scale solar thermal electric systems [8]. CSP plants can use a half-dozen different technologies, but the four best suited for use in ISCC power plants are:

1. Parabolic troughs

2. Compact linear Fresnel collectors

3. Parabolic Dishes

4. Central Receivers (Solar Tower technology)

From these technologies, the parabolic trough and the solar tower are competitive and economically feasible. In this study, we chose the solar tower technology with molten salt as the HTF. The solar tower thermal power generation is one the most promising technologies for producing solar electricity on a large scale. Not only is it one the least expensive methods to produce solar electricity, it also achieves extremely high concentration of solar radiation resulting in high thermodynamic performances. Direct solar radiation is concentrated up to 1000 times by using reflective mirrors, called heliostats, onto a receiver placed at the top of a tower. The solar flux is then transferred to a HTF running through the tubes of the receiver.

The solar tower power plant consists of the following subsystems and components: the heliostat field, tower and receiver, TES (optional), duct burner (optional), power conversion system, plant control, auxiliary power supply and heat rejection [9]. Of all the above, the heliostat field is possibly the most important subsystem because it typically contributes to ~50% of the total cost of the system and causes ~47% power losses [10]. These numbers indicate that particular attention must be given to the development and optimization of low cost and high efficiency heliostat field layouts.

The heliostat fields studied in this paper were created with an algorithm written in Fortran95 and C#. The methodology was based on DELSOL's studies. Some adjustments were made with the help of Siala's paper [9] as well as a series of papers by Changchun Institute of Optics and the Key Laboratory of Solar Thermal Energy and Photovoltaic System [10, 11, 12], both located in China.

Our algorithm follows the radial staggered distribution. It locates the heliostats in the field of a solar central receiver plant so that they provide no blocking losses over the years. While the method makes sure that neighboring heliostats block none of the reflected sunlight, it does not take into consideration any shadowing losses because they are of less significance in comparison to blocking losses.

The heliostat field boundary is constrained by the tower height and the receiver geometrical aperture. The receiver aperture in our design has a circular shape, therefore its projection boundary on the field is an ellipse.

Before we explain the methodology of the algorithm we define the following terms:

- Essential Ring: the ring has a heliostat on the north axis of the field
- Staggered Ring: the ring has no heliostat placed on the north axis
- Azimuthal Spacing: the safe distance between two consecutive heliostats of the same ring that allows them to move without mechanical interference.
- Radial Spacing: the distance needed in order to minimize blocking of the reflected beams between heliostats of the same angular direction, either essential or staggered.

The algorithm's procedure is summarized in the following steps:

1) Takes as input the desired tower height, receiver tilt angle and heliostat dimensions

2) The first ring of heliostats is placed on a radius, with length 0.8*(aim point height), in front of the tower

3) Each heliostat is marked as a circle with a diameter equal to DM= $\sqrt{HM^2 + WM^2}$ (1)

4) The heliostats in each ring are separated by an azimuthal spacing, $\mathrm{DA} = \mathrm{WM}^*(1,749 + 0,6369 * \theta_L) + \frac{0,2873}{\theta_L - 0,04902}$, where $\theta_L = \tan^{-1}(\frac{THT}{R})$ (2)

5) After placing the heliostats in the first ring we check whether it is possible to place another heliostat between each pair of heliostats. This is done with a loop until no more heliostats can be placed

6) The radius of the second ring (staggered) is determined as the nearest distance, to the first ring sufficient to prevent interference between the two rings.

7) Heliostats are placed in the second row with the same criteria as in the first ring.

8) The second essential ring (or the third ring in row) is placed on a radial distance from the previous essential ring, $\mathrm{DR} = H\ \mathrm{M}^*(1,44 * \cot\theta_L - 1,094 + 3,068 * \theta_L - 1,1256 * \theta_L{}^2)$ (3)

9) The above steps are repeated until the last ring, whose radius is 7.15*(aim point height)

10) The elliptical projection of the receiver's aperture is also marked on the field. The heliostats enclosed in the ellipse are the ones we keep, while the rest are discarded.

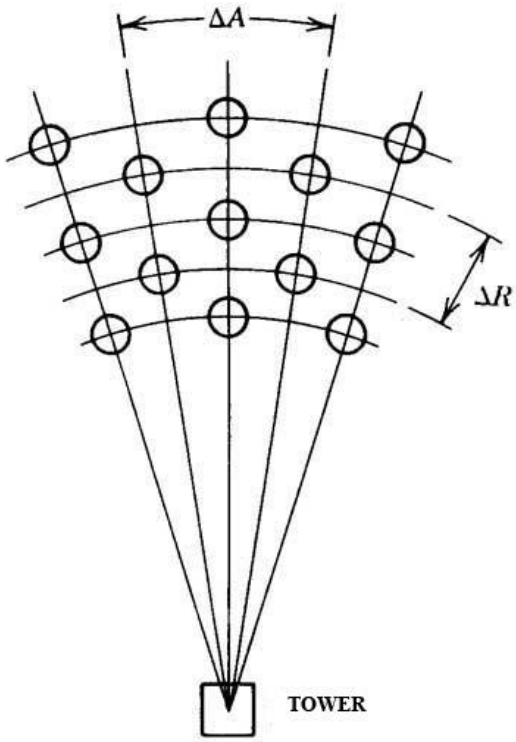


*Figure 5. Azimuthal and Radial Spacing [13]*

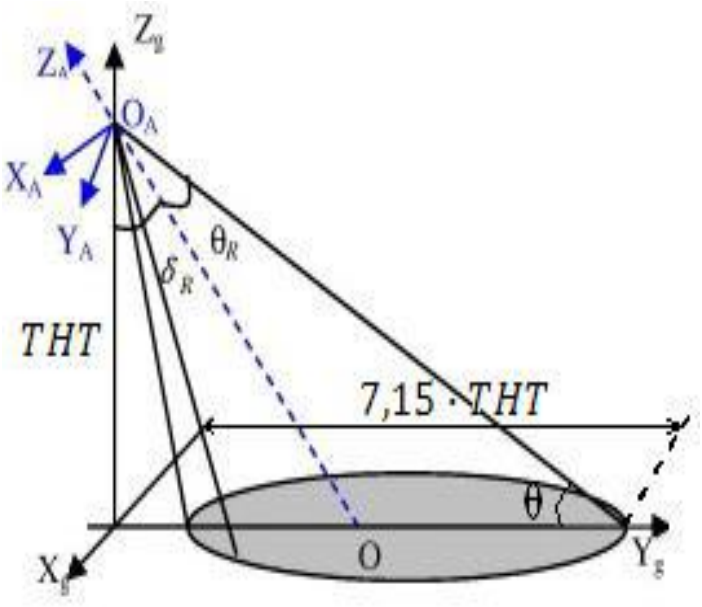


*Figure 6. Heliostat field boundaries[10]*

## 4. Solar Integration & Thermodynamic Results

Through the solar integration we aim to substitute the use of certain heat exchangers, when this is feasible based on the solar energy extracted from the heliostat field, without letting the output temperature of the exhaust gas increase. We also, wanted to examine whether it is possible to reduce the mass of the exhaust gas, and consequently the consumed mass of the natural gas.

In the first scenario we substitute the SH-HP-1 and SH-LP heat-exchangers. In the second one, the SH-MP-1 and SH-LP exchangers and in the third one the SH-HP-1 and SH-MP-1.

For each region we created a total of 36 possible field layouts. Three different tower heights (145m, 165m and 185m), four different receiver tilt angles ($0^o$, $20^o$, $40^o$ and $60^o$) and three different heliostat dimensions (9x13, 10x12, 11x11) were chosen.

The computations were performed for two representative days of the year, the first one with relatively high solar radiation and the second one with weak solar radiation, a quite commonly used method for studies that involve solar power, since it provides adequate results without the need for excessive data input [14][15][7][16].

After calculating the solar energy gain for the summer period, the three scenarios that meet the thermal needs of the fore mentioned heat exchangers to be substituted are the following, for Thisvi's power plant:

-Tower 145m, Receiver tilt angle 40$^{o}$, heliostat dimensions 11x11, producing 45.357 MW (SH-HP-1 and SH-LP)

-Tower 165m, Receiver tilt angle 60$^{o}$, heliostat dimensions 9x13, producing 31.063 MW (SH-MP-1 and SH-LP)

-Tower 145m, Receiver tilt angle 20$^{o}$, heliostat dimensions 9x13, producing 63.393 MW (SH-HP-1 and SH-MP-1)

Similarly, the following scenarios were chosen for Cyprus:

-Tower 185m, Receiver tilt angle 60$^{o}$, heliostat dimensions 9x13, producing 48.450 MW (SH-HP-1 and SH-LP)

-Tower 145m, Receiver tilt angle 60$^{o}$, heliostat dimensions 11x11, producing 31.606 MW (SH-MP-1 and SH-LP)

-Tower 165m, Receiver tilt angle 40$^{o}$, heliostat dimensions 9x13, producing 67.952 MW (SH-HP-1 and SH-MP-1)

Based on the above scenarios our TES was designed for four cases: 3h, 6h, 9h and 12h depending on the DNI value and hours of sunshine. The overall hours of irradiance per year, are 2518 for Thisvi and 3194,83 for Cyprus.

After the solar integration, the new fuel consumption, the percentage of power originating from the solar tower and the new CO2 emissions were estimated. The same computations were made for the winter period. Finally, using a weighted average fuel consumption for summer and winter, the annual fuel savings, the renewable MWh and the total CO2 emissions were calculated.

As mentioned above three different network configurations of the thermal-solar system were examined, but for the purposes of this paper only the one that intervenes in MP and LP is being presented. Figures 7a and 7b illustrate the new Q-T diagrams composed for both the summer and winter period.

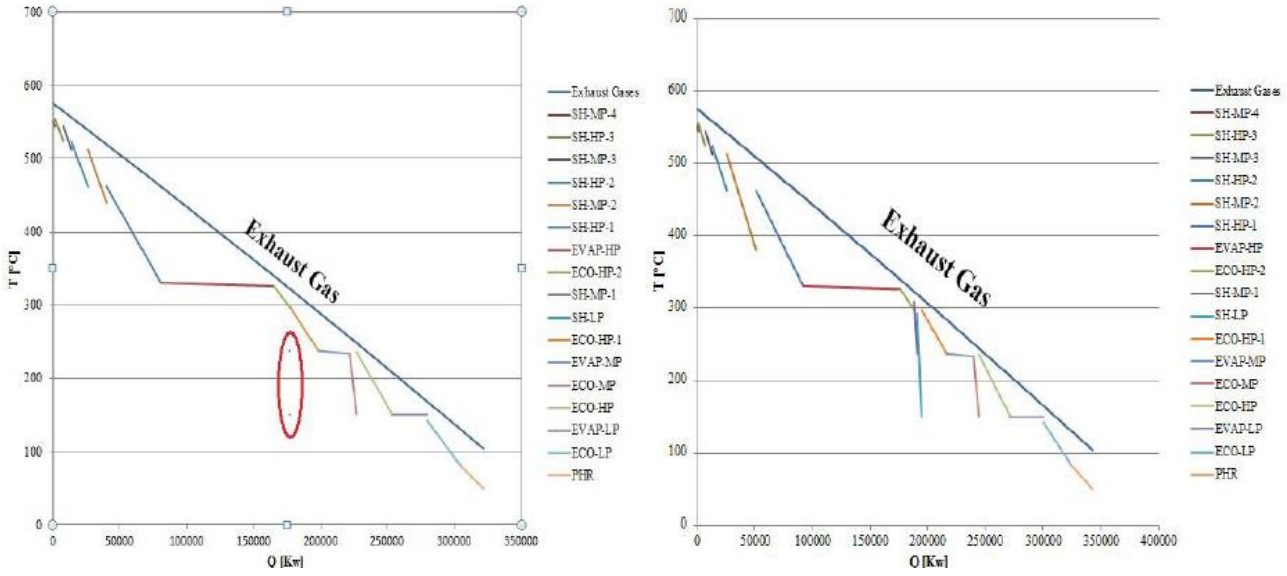


*Figure 7 (a,b). Q-T diagram for summer and winter period*

.The energy and exergy efficiencies of the ISCC of every case are summarized in tables (3a) and (3b)

*Table 3a. Energy efficiency Results*

| Configuration | Energy Efficiency % |
|---|---|
| Current | 57.93 |
| HP-LP summer | 56.40 |
| HP-LP winter | 57.56 |
| MP-LP summer | 57.03 |
| MP-LP winter | 57.71 |
| HP-MP summer | 55.68 |
| HP-MP winter | 57.26 |

*Table 3b. Exergy efficiency results*

| Configuration | Exergy Efficiency % |
|---|---|
| Current | 55.25 |
| HP-LP summer | 56.72 |
| HP-LP winter | 55.39 |
| MP-LP summer | 56.20 |
| MP-LP winter | 55.46 |
| HP-MP summer | 56.86 |
| HP-MP winter | 55.32 |

Moreover these results may be more comprehensible if the energy flow and the exergy destruction are illustrated by Sankey and Grassmann diagrams respectively.

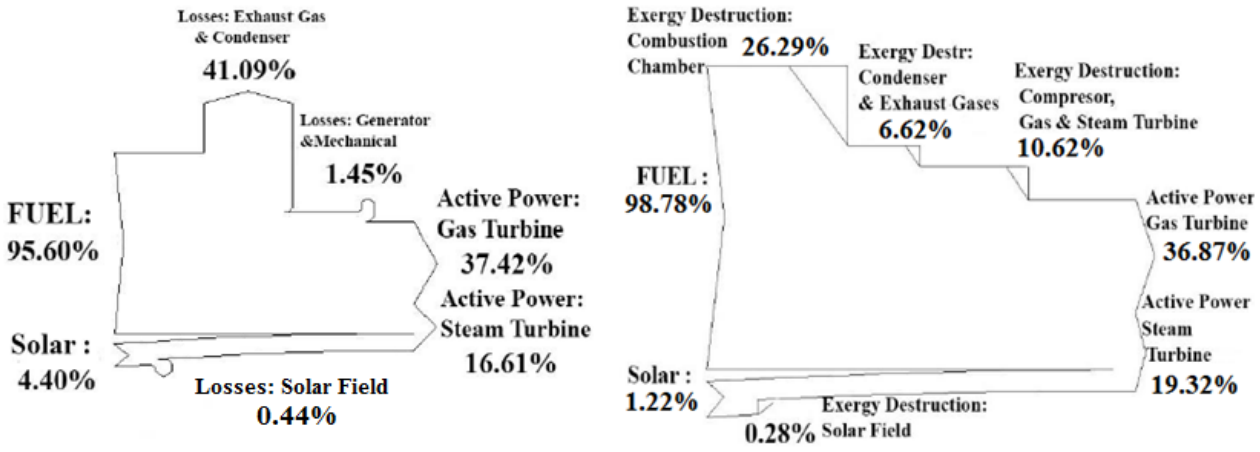


*Figure 8 (a,b) Sankey and Grassmann diagram for summer period*

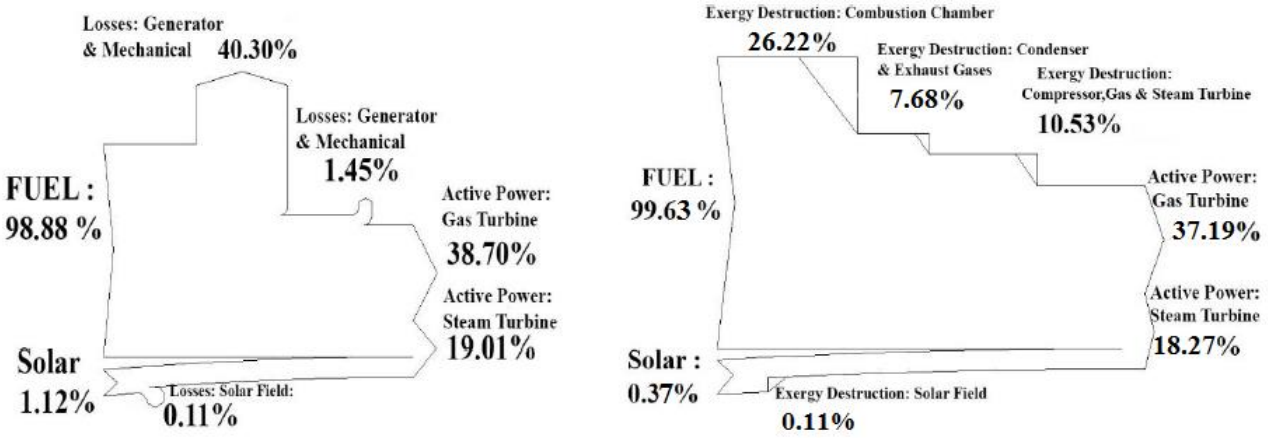


*Figure 9 (a,b) Sankey and Grassmann diagram for winter period*

*Table 4 (a,b). Exergy destruction of the components for summer and winter period*

| Component | Exergy Destruction % |
|---|---|
| Gas Turbine | 6.34 |
| Compressor | 2.97 |
| Steam Turbine | 1.31 |
| Condenser | 2.42 |
| Exhaust Gases | 4.20 |

| Component | Exergy Destruction % |
|---|---|
| Gas Turbine | 6.32 |
| Compressor | 2.96 |
| Steam Turbine | 1.25 |
| Condenser | 2.31 |
| Exhaust Gases | 5.37 |

### 4.1.Discussion

In figures 7a and 7b is easily observed that the two heat exchangers which had been fully or partly substituted, in these two periods, are the SH-MP-1 and SH-LP. It is also obvious that during winter, the solar field's contribution is negligible and as a result the heat exchanger SH-MP-1 operates as before the solar integration.

Additionally both of the exhaust gas heat curves are steeper than the existing (figure 3) due to the reduction of fuel consumption and the solar thermal gain. The Q-T also depicts the energy and exergy utilization of the exhaust gases from the HRSG and the overall power plant.

In addition figures 8a and 8b illustrate that there is a 3 % difference in power rate enhancement from the solar field between these two periods, whereas the active power rate remains almost equal.

Table (3a) remarks that the existing situation has the highest energy efficiency. During winter the three different configurations approach this result, whereas during summer there is a slight decrease. These results were quite expected, because in summer period there is a greater supply of power from the solar thermal system, less consumption of fuel than in winter and the net power from the steam turbine is the same in both periods. It is noted, that there is linear correlation between the power from the GT and the fuel consumption.

In contrast, table (3b) shows that the HP-MP configuration is the one that disposes the highest and the lowest exergy efficiency during summer and winter respectively. Apparently during summer the efficiency is constantly higher than in winter in every case, thus for lower fuel consumption the exergetic destruction is also lower.

As for the presented case, there are no particular differences in exergy efficiency between these periods. Nonetheless, tables 4a and 4b remark that there is a significant difference in exergy destruction due to the exhaust gases (4.20 % during summer period while 5.37% during winter period).

Furthermore, it is observed that the combustor of the gas turbine is the major part of exergy losses with 26.29% and 26.22 % for summer and winter period respectively, a fact that was also evaluated in other similar studies [17][18] .

On the other hand, the exergy production from the solar field is 1.12% in summer (to overall exergy), but is reduced to 0.37 % in winter. This gap is fulfilled by the consumed natural gas.

Finally, there is an interesting alternation in the active power rate production of GT and ST, i.e. in summer the ST power rate production is greater than in winter the reverse is observed for the GT power rate production.

## 5. Economic evaluation of the investment

In this section the investment evaluation for both countries, is presented. For this purpose the following economic indicators were calculated: PV, NPV, IRR, discounted payback period, the extra LEC [19] and the covetable feed in tariff for exact 5 years discounted period payback.

For the existing case a 4000 hr/year operational time was assumed, whereas the three new configurations were operating during the hours of irradiance and TES as a hybrid system and the rest of the year as a conventional CCPP. Nevertheless, there were circumstances when the 4000 hr/year operational time was exceeded because of the TES. In these cases the overall operational time, for every intervention, was the one that accrued from the hours of the irradiance and TES.

It was also assumed that the financing was 100 % equity and the interest rate 9 %. The selling price for the conventional power was taken 60 €/MWh [20], whereas a feed in tariff 284.85 €/MWh was taken for the power generated from the solar thermal system with at least 2 hours TES and 264.85 €/MWh without TES [21]. Finally the cost of natural gas was assumed 0.04 €/Kwh [22] and the cost of $CO_2$ 7.5 €/tn [23].

The cost of the investment's components is presented in table (4)

*Table 5. Cost of solar field's components [24], [25], [26],[27]*

| Component | Cost |
|---|---|
| Heliostats | 110 €/m$^2$ |
| Land use | 5 €/m$^2$ |
| TES | 36 €/KWth |
| Solar salt | 1 €/kg |
| O&M | 1.5 % Capital Cost |

For the calculation of the solar tower and the receiver costs the following exponential expressions were used [28]:

$$I_{Tow} = I^o_{Tow} \cdot \left( \frac{H_{Tow}}{H^o_{Tow}} \right)^{S_{Tow}} \cdot \left( pr_{Tow} \right)^{\log_2 \frac{V_{Tow}}{V^o_{Tow}}} \cdot pi_{Tow} \quad (4)$$

$$I_{\mathrm{Re}c} = I^o_{\mathrm{Re}c} \cdot \left( \frac{A_{\mathrm{Re}c}}{A^o_{\mathrm{Re}c}} \right)^{S_{Tow}} \cdot \left( pr_{\mathrm{Re}c} \right)^{\log_2 \frac{V_{\mathrm{Re}c}}{V^o_{\mathrm{Re}c}}} \cdot pi_{\mathrm{Re}c} \quad (5)$$

Where:

$H_{Tow}[m]$ $\quad$ $V_{Tow} = [unit]$

$I^o_{Tow} = 1.6[M\$]$ $\quad$ $H^o_{Tow} = 75[m]$

$s_{Tow} = 1.797 I^o_{Tow}$ $\quad$ $pr_{Tow} = 0.9526$

$V^o_{Tow} = 1[unit]$ $\quad$ $pi_{Tow} = 1.030501$

$\mathrm{A}_{\mathrm{Re}c}[m^2]$ $\quad$ $V_{\mathrm{Re}c} = [unit]$

$I^o_{\mathrm{Re}c} = 9.1[M\$]$ $\quad$ $A^o_{\mathrm{Re}c} = 100[m^2]$

$s_{\mathrm{Re}c} = 0.5283$ $\quad$ $pr_{\mathrm{Re}c} = 0.9526$

$V^o_{Tow} = 1[unit]$ $\quad$ $pi_{\mathrm{Re}c} = 1.030501$

Finally, all economic indicators are depicted in the following figures:

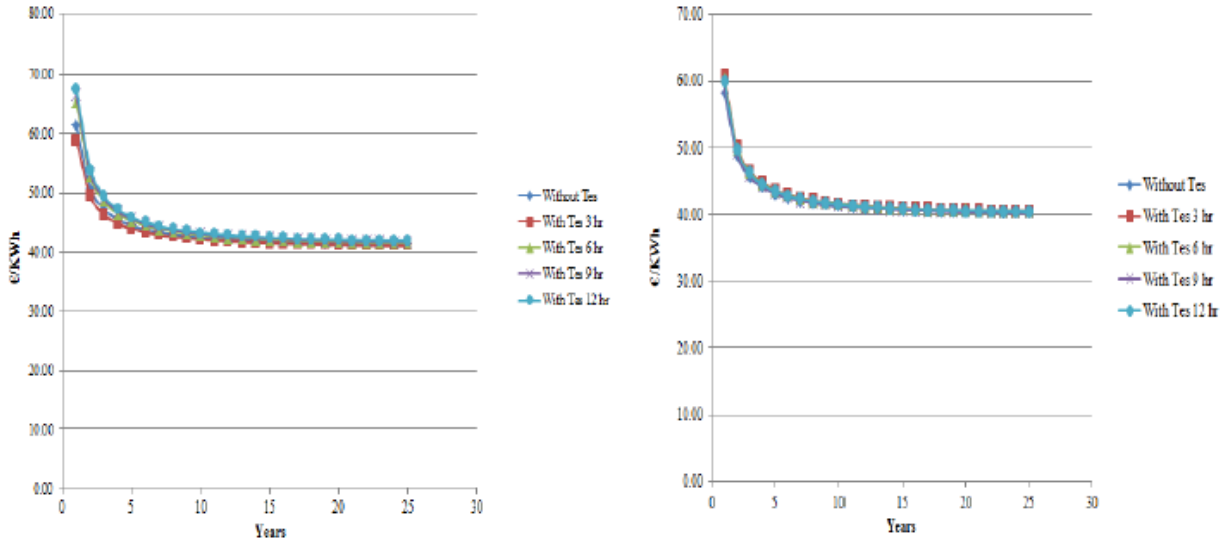


*Figure 10 (a,b) The extra LEC for Thisvi and Cyprus*

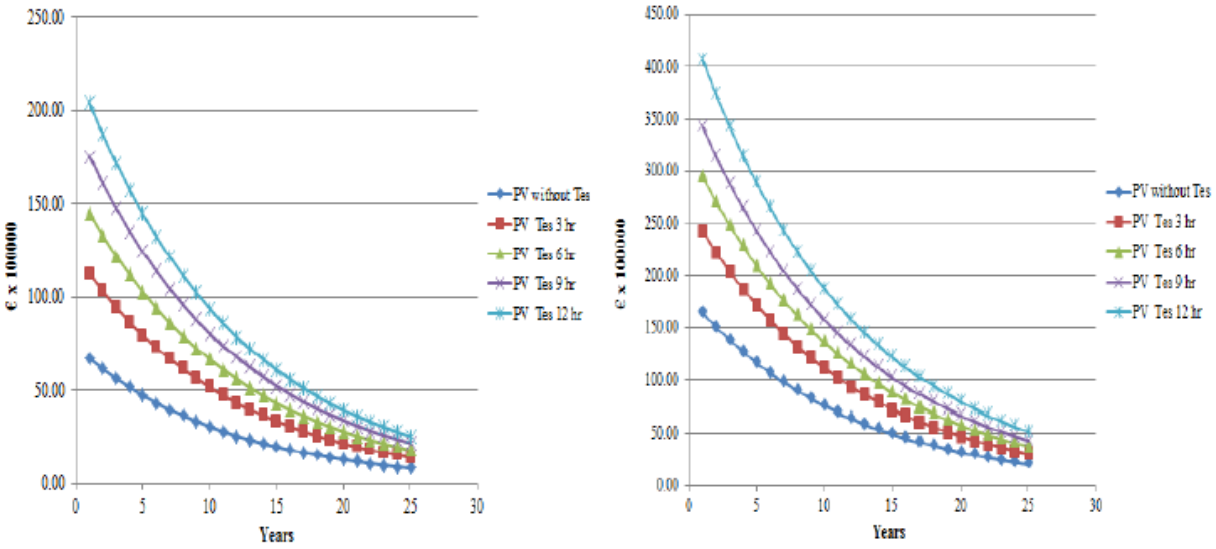


*Figure 11 (a,b) The PV for Thisvi and Cyprus*

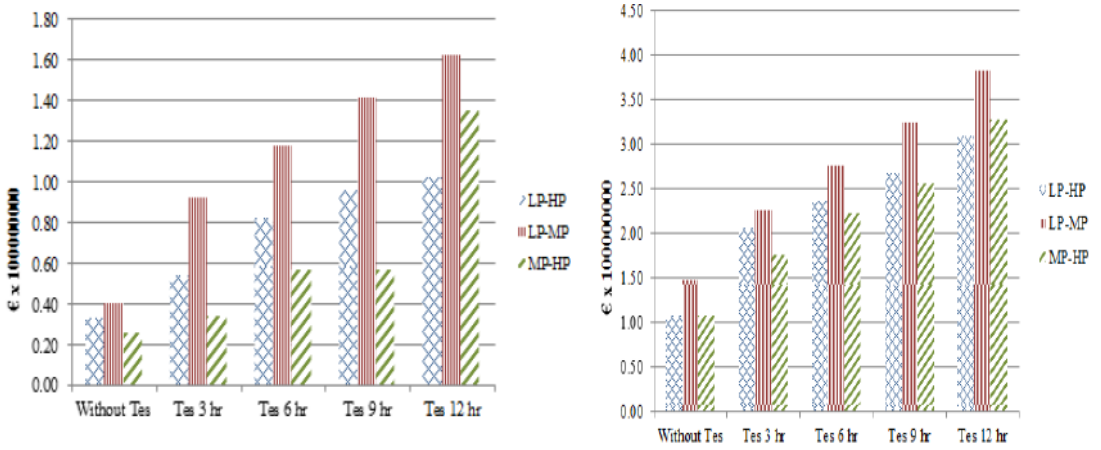


*Figure 12 (a,b) The NPV for Thisvi and Cyprus*

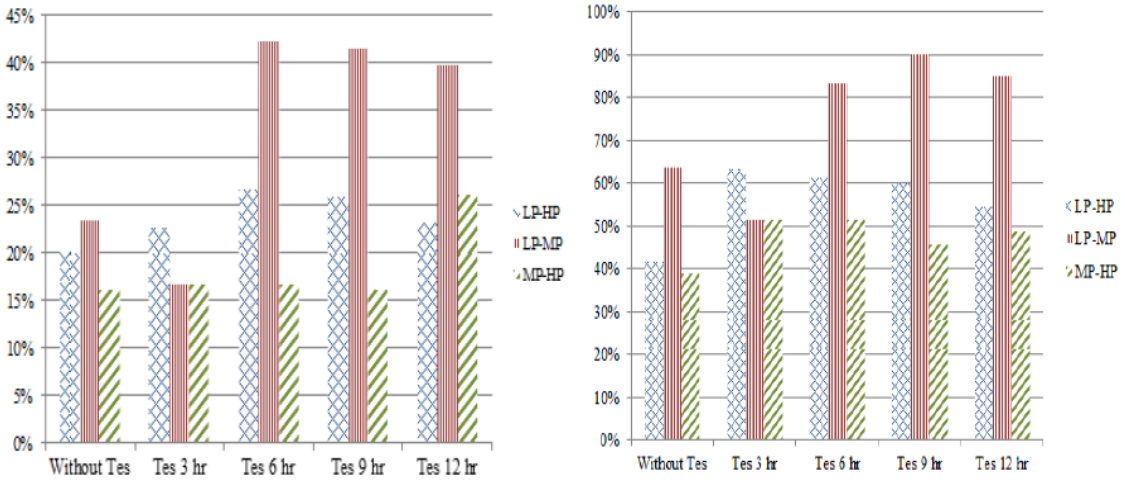


*Figure 13 (a,b) The IRR for Thisvi and Cyprus*

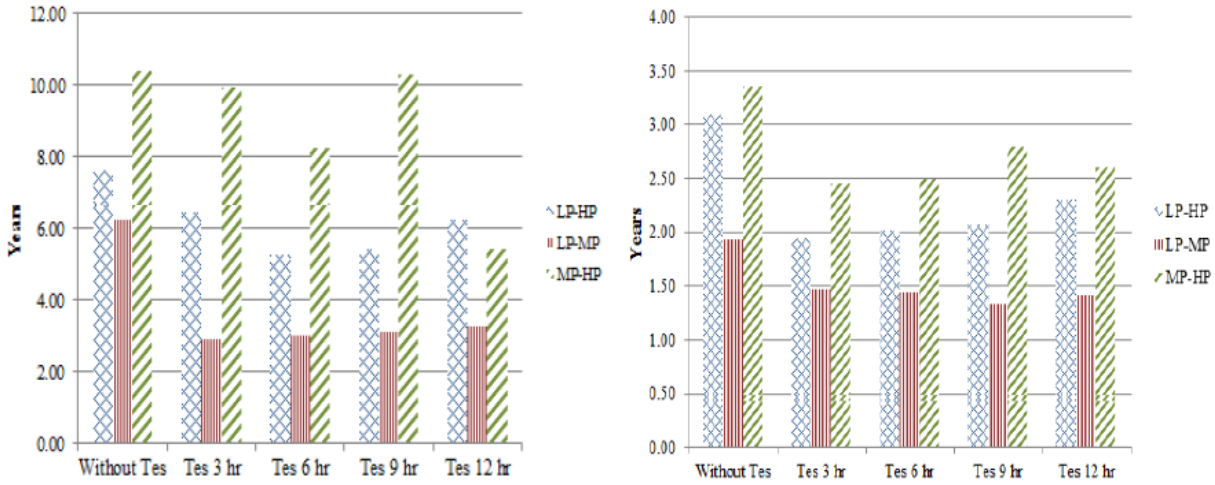


*Figure 14 (a,b) The discounted payback period for Thisvi and Cyprus*

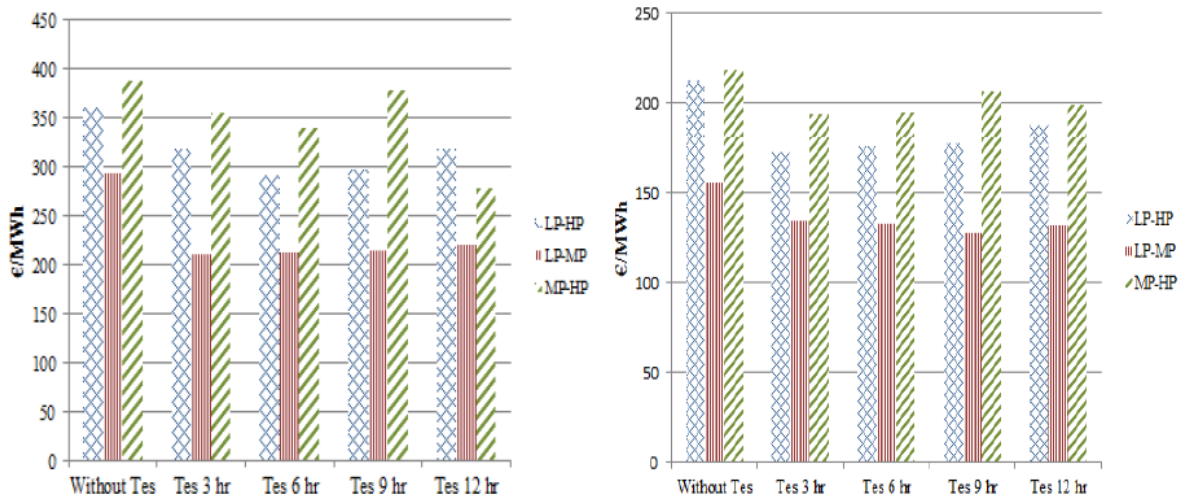


*Figure 15 (a,b) The cost of MWh for exact 5 years payback for Thisvi and Cyprus*

## 6. Conclusions

It is quite obvious from all the above figures that the most efficient investment is the one that intervenes in MP and LP, due to the low capital cost of the investment. Finally, comparing all the above economic indicators of these two regions (Thisvi and Cyprus) we concluded that the investment is safer in Vasiliko of Cyprus in every single scenario as result of the region's higher DNI values. Although the existing situation has the highest energy efficiency, the investment offers many benefits: decrease in CO2 emissions, fuel consumption savings and reasonable payback time. In terms of future study, we recommend the employment of a different HTF and possibly the use of DSG, in which steam is produced directly from the solar receiver, without using HTF and heat exchangers, aiming to achieve lower capital costs , energetic and exergetic losses [15].

## References

[1]Antonio Rovira, María José Montes, Fernando Varela, Mónica Gil, Comparison of Heat Transfer Fluid and Direct Steam Generation technologies for Integrated Solar Combined Cycles, Applied Thermal Engineering 52 (2013) 264-274

[2] Jürgen Dersch, Michael Geyer, Ulf Herrmann, Scott A. Jones, Bruce Kelly, Rainer Kistner, Winfried Ortmanns, Robert Pitz-Paal, Henry Price Trough integration into power plants - a study on the performance and economy of integrated solar combined cycle systems

[3] R. Hosseini, M. Soltani, G. Valizadeh .Technical and economic assessment of the integrated solar combined cycle power plants in Iran

[4]Guangdong Zhu, Ty Neises; Craig Turchi, Robin Bedilion, Thermodynamic Evaluation of Solar Integration into a Natural Gas Combined Cycle Power Plant

[5] Mechthild Horn, Heiner Führing, Jürgen Rheinländer, Economic analysis of integrated solar combined cycle power plants, A sample case: The economic feasibility of an ISCCS power plant in Egypt

[6]Spiros Alexopoulos, Bernhard Hoffschmidt, Solar tower power plant in Germany and future perspectives of the development of the technology in Greece and Cyprus, Renewable Energy 35 (2010) 1352–1356

[7] Yuanyuan Li, Yongping Yang. Thermodynamic analysis of a novel integrated solar combined cycle. Applied Energy 122 (2014), 133–142

[8] David Kearney, Fred Morse, Bold, decisive times for concentrating solar power. Sol Today, 24 (4) (2010), pp. 32–35

[9]F.M.F. Siala, M.E.Elayed, Mathematical formulation of a graphical method for a no-blocking heliostat field layout, Renewable Energy 23 (2001) 77-92

[10]Xiudong Wei, Zhenwu Lu, Weixing Yu, Zhifeng Wang, A new code for the design and analysis of the heliostat field layout for power tower system, Solar Energy 84 (2010) 685-690

[11]Xiudong Wei, Zhenwu Lu, Weixing Yu, Zhifeng Wang, Hongxing Zhang, Zhihao Yao, A new method for the design of the heliostat field layout for solar tower, Renewable Energy 35 (2010) 1970-1975

[12]Xiudong Wei, Zhenwu Lu, Zi Lin, Hongxing Zhang, Zhengguo Ni, Optimization procedure for Design of Heliostat Field Layout of a 1MWe Solar Tower Thermal Power Plant

[13] http://www.powerfromthesun.net/Book/chapter10/chapter10.html

[14] G. Franchini, A. Perdichizzi, S. Ravelli , G. Barigozzi. A comparative study between parabolic trough and solar tower technologies in Solar Rankine Cycle and Integrated Solar Combined Cycle plants. Solar Energy 98 (2013), 302–3.14

[15] Omar Behar , Abdallah Khellaf , Kamal Mohammedi , Sabrina Ait-Kaci. A review of integrated solar combined cycle system (ISCCS) with a parabolic trough technology. Renewable and Sustainable Energy Reviews 39 (2014 )223–250

[16] Yawen Zhao, Hui Hong, Hongguang Jin. Mid and low-temperature solare coal hybridization - mechanism and validation. Energy 74 (2014). 78-87

[17] Baghernejad A,Yaghoubi M. Exergy analysis of an integrated solar Combined Cycles system . Renew Energy 35 (2010) . 2157–2164.

[18] Siva Reddy V, Kaushik SC, Tyagi SK. Exergetic analysis of solar concentrator aided natural gas fired combined cycle power plant. Renewable Energy 39 (2012), 114–125.

[19] H. Nezammahalleh, F. Farhadi , M. Tanhaemami. Conceptual design and techno-economic assessment of integrated solar combined cycle system with DSG technology. Solar Energy 84 (2010), 1696–1705

[20]http://www.lagie.gr/agora/analysi-agoras/miniaia-deltia-iep/

[21] Greek Government's Newspaper .3851 Law.(2010), 85

[22] G.C. Bakos, D. Parsa. Technoeconomic assessment of an integrated solar combined cycle power plant in Greece using line-focus parabolic trough collectors. Renewable Energy 60 (2013),598-603

[23] E-ntelligence, Energy and Emissions consultants

[24] Antoni Gil, Marc Medrano, Ingrid Martorell, Ana La´zaro, Pablo Dolado, Bele´n Zalba ,Luisa F. Cabeza. State of the art on high temperature thermal energy storage for power generation. Part 1—Concepts, materials and modellization. Renewable and Sustainable Energy Reviews 14 (2010),31–55

[25] D. Kearney , B. Kelly , U. Herrmann , R. Cable , J. Pacheco ,R. Mahoney , H. Price , D. Blake , P. Nava , N. Potrovitza . Engineering aspects of a molten salt heat transfer fluid in a trough solar field. Energy 29 (2004) 861–870

[26] http://opensourceecology.org/wiki/Heliostat

[27] International Renewable Energy Agency. RENEWABLE ENERGY TECHNOLOGIES: COST ANALYSIS SERIES. Concentrating Solar Power. June 2012

[28] C. Ballif, D. Favrat, V. Aga, M. Romero, A. Steinfeld, Germain Augsburger. Thermo-economic optimisation of large solar tower power plants. Suisse 2013